CONF-9211129--2

IAEA SODIUM VOID REACTIVITY BENCHMARK CALCULATIONS

R. N. Hill and P. J. Finck
Reactor Analysis Division
Argonne National Division
Argonne, IL 60439 (USA)

DISCLAIMER

To be presented at: IAEA Consultancy
Vienna, November 1992

ANL/RA/CP--78050

DE93 004849

I. INTRODUCTION

In the aftermath of the Chernobyl accident, there has been renewed interest in designing LMR cores with a low sodium void worth [i.e., ref.1]. Although large margins between the peak coolant temperature and sodium boiling temperature have been demonstrated in fast reactors for various unprotected transients, there remains a non-zero probability of at least a limited amount of sodium voiding in a LMR. Several mechanisms have been postulated that could lead to limited voiding; these mechanisms include sodium boiling conditions caused by local flow blockages and gas insertion conditions caused by fission gas release or cover gas entrainment. Moreover, the possibility of large-scale voiding as a result of extremely unlikely events cannot be entirely dismissed; and in conventional fast reactor designs, large-scale voiding would introduce substantial positive reactivity which could potentially lead to reactor damage.

For all of the above reasons, there remains a strong incentive to minimize the sodium void worth and the consequent potential for reactor damage in the extremely unlikely event that voiding takes place. However, as pointed out in reference 1, reduction of the void worth is achieved at the expense of performance, design, and possibly safety penalties; thus, the usefulness of void worth reduction options must be evaluated in the context of overall safety of the reactor system [2]. Recently, a number of low void worth core designs with non-conventional core geometries have been proposed. Since these designs lack a good experimental and computational database, benchmark calculations are useful for the identification of possible biases in performance characteristic predictions.

Many of the design changes applied in low void worth designs (i.e., enhanced leakage characteristics) create physical phenomena which may not be accurately modeled by conventional reactor physics computational methods. Moreover, the principal attribute of these designs (the near-zero void worth) arises from the compensation of a large (positive) spectral effect and a large (negative) leakage effect; thus, accurate physics prediction are especially difficult. Previous benchmark comparisons [3] assessed the performance predictions for a metal-fueled core design in which a low void worth was reduced by utilizing a pancaked, annular core geometry. For four distinct core compositions, the flooded and voided multiplication factor, power peaking factor, sodium void worth (and its components), flooded Doppler coefficient, control rod worths, yearly burnup reactivity swing, average discharge burnup, peak linear power, and fresh fuel enrichment predictions of two independent evaluations were compared. In general, remarkably good agreement was observed in the performance predictions. However, a significant bias of 0.3-0.5 % $\Delta k/(kk')$ in the sodium void worth was observed.

In this paper, the IAEA-1992 "Benchmark Calculation of Sodium Void Reactivity Effect in Fast Reactor Core" problem is evaluated. The proposed design is a large axially heterogeneous oxide-fueled fast reactor as described in Section 2; the core utilizes a sodium plenum above the core to enhance leakage effects. The calculation methods

used in this benchmark evaluation are described in Section 3. In Section 4, the calculated core performance results for the benchmark reactor model are presented; and in Section 5, the influence of steel and interstitial sodium heterogeneity effects is estimated.

II. BENCHMARK MODEL DESCRIPTION

The 1992 IAEA benchmark model is a simplified three-dimensional calculational model of a Russian BN-800 type reactor of 2100 MWt power output. In this design, the sodium void worth has been reduced to near-zero by the introduction of a special sodium plenum above the core with a low steel content (<10%). The voiding of this plenum zone gives a large negative (leakage) reactivity effect because of the degraded neutron reflection in the voided state; this negative reactivity effect compensates the positive reactivity effect of the fueled region.

The benchmark model geometry and material composition was described in detail in the IAEA benchmark specification document [4]. The core design is an axially heterogeneous configuration with two distinct driver zones. An 18.2 cm thick central axial blanket is utilized in the inner core, and power peaking is reduced by removing the axial blanket in the outer core. External breeding regions include a thick (40.5 cm) axial blanket below the active core and a single row of radial blankets surrounding the core. Three rows of radial shielding are utilized beyond the radial blanket (a single row of steel shield subassemblies and two rows of boron carbide shield subassemblies). Two distinct control systems are utilized (eighteen compensating rods and twelve safety rods); the control assemblies are evenly spaced within the inner core zone. Forty-one distinct material compositions and their spatial locations are specified in reference 4. For the benchmark comparisons, six different voided states were specified. The first three cases evaluate voiding in the driver assemblies alone; progressive axial voiding of the active core, upper sodium plenum, and upper axial blanket is evaluated. The second three cases evaluate subsequent sodium voiding in the control assemblies in a similar manner. For the maximum void state, the regional and reaction-wise components of the void worth will be evaluated. In addition to the void worth calculations, radial and axial power distribution, control rod worth, and breeding characteristic evaluations were proposed. The calculational problems of steel heterogeneity in the sodium plenum and interstitial sodium contribution to the total void worth are estimated based on a heterogeneous assembly model also specified in reference 4.

III. DESCRIPTION OF CALCULATIONAL METHODS

Group constants were generated from ENDF/B-V.2 using the MC^2-2/SDX code package [5,6] for an oxide fuel composition with an enrichment of 23.8% Pu/HM. Group constants were evaluated at typical operating temperatures (fuel - 1300K, structure - 750K, coolant - 700K in the driver; fuel - 950K, structure - 725K, coolant - 700K in the blanket, and all materials 650K in non-fueled regions). Region-dependent group constants were spatially collapsed to a 21 energy group structure using a 230 group regional flux distribution from a one-dimensional model of a radially heterogeneous layout. Group constants were generated separately for sodium-in and sodium-out cases.

Conventional computations of the flux and adjoint flux distributions were performed using finite difference diffusion theory; a power normalization factor of 200 MeV/fission as specified in reference 3 was utilized. The void worth and its components were calculated using exact perturbation theory. In the depletion case, regional core composition changes were modeled using the REBUS-3 code [7]; the regional depletion was calculated for each composition zone specified in the benchmark model using 9 energy group cross sections and a depletion time of 30 days.

In addition to the conventional diffusion theory results, the effect of several higher order methods was also evaluated. For selected cases, the void worth was evaluated using a full core VIM [8] Monte Carlo model at room temperature. The VIM calculation utilizes a continuous energy representation of the cross section data; however, lumped fission product data is not fully validated in the current VIM library, and corrections for fission products were obtained from 3D multigroup transport calculations. The void worth was also evaluated using the hex-Z variational nodal transport theory code VARIANT [9, 10, 11, and description below] and the nodal diffusion option of the DIF3D code [12]. The heterogeneous assembly model was evaluated using the VIM code exclusively. Typical running time for diffusion calculations on an IBM RISC workstation was around 180 seconds. On a SUN Sparc-2 workstation, roughly 20 Monte-Carlo histories can be obtained for every CPU second for a full core fast reactor model; thus, a typical calculation (10 million histories) can be obtained in roughly 6 CPU days. Note that actual time can be significantly reduced by distributing the calculations over several workstations.

VARIANT is based on the variational nodal method, and solves the multigroup transport equation using a response matrix formalism. Complete polynomial expansions up to fourth order are used to represent the flux distribution within the node; currents are expanded up to the second order. The angular dependence of the flux and currents are represented by spherical harmonics of order P_3. VARIANT is currently being extensively verified and validated by comparison to higher order transport methods (discrete ordinates and Monte Carlo); these comparisons usually show very good agreement for predicted eigenvalues, fluxes, and power densities.

Two options of VARIANT were used: a simplified version [10] exists, which uses transport corrected P_0 scattering matrices and a reduced set of angular trial functions, and gives results similar to typical 3D transport codes used elsewhere (~80% of the true multigroup transport effect); a more advanced version[11] explicitly treats anisotropic scattering up to order P_3, and uses a full set of angular trial functions, and has been shown to reproduce almost 100% of the true multigroup transport effect. Whereas the simplified version requires ~1 CPU hour on a typical IBM RISC workstation for a typical fast reactor problem and can be routinely used for scoping calculations, the more advanced version still requires several hours of CPU, and is used only for benchmarking purposes.

IV. BENCHMARK RESULTS AND DISCUSSIONS

Benchmark results are given in the following tables and figures:

- Figure 1 represents the peak power density by assembly at the lower core mid-plane for the flooded core configuration. These values can be converted to maximum linear powers (W/cm): the conversion factor is 0.69.

- Figure 2 represents the peak power density by assembly at the upper core mid-plane for the flooded core configuration.

- Figure 3 represents the axial distribution of the peak power density in the central subassembly for the flooded core configuration.

- Figure 4 represents the axial distribution of the peak power density in a peripheral core subassembly for the flooded core configuration.

- Table I gives the core eigenvalue for one flooded and six voided cases, calculated with various methods: finite differences (triangular-Z) diffusion theory, nodal (Hex-Z) diffusion theory, nodal (Hex-Z) transport theory with P_0 transport corrected scattering matrices and a reduced set of angular trial functions, and nodal (Hex-Z) transport theory with P1 scattering matrices and a full set of angular trial functions. All these calculations explicitly take into account the fission products.

- Table II gives the core eigenvalue for the same seven cases, using finite differences diffusion theory, nodal transport (P_0 scattering) and continuous energy Monte Carlo (using 20 million histories for the flooded case, and 10 million histories for each of the three voided cases, the one sigma uncertainties are shown). These calculations do not take into account the fission products: this was done because VIM does not currently have a well validated fission product model.

- Figure 5 summarizes these void worth results: it gives for each successive voiding case, the eigenvalue change from the flooded case. Note that the VIM continuous energy Monte Carlo results have been corrected for the effect of fission products: the correction was obtained from the differences of the nodal transport results (P_0 scattering) with and without fission products. The Monte Carlo results are given within a plus or minus three sigma uncertainty band.

- Table III gives an exact perturbation breakdown of the regional and reaction-wise components for the maximum voiding case. Note that this result was obtained from a diffusion theory calculation and probably has limited validity in view of the large transport effects observed for this sodium voiding problem; unfortunately, no perturbation code is currently available to analyze 3D transport predictions;

- Table IV summarizes the core neutronic performance characteristics: breeding ratios, burnup swing, peak linear power, power peaking factor, regional power fractions, and control rod worths.

The most significant results are illustrated in Figure 5: all methods indicate a large positive void worth of 1.2-1.5 % $\Delta k/(kk')$ in the active core region which is compensated by a large negative reactivity effect when the sodium plenum is voided (giving a near-zero net void worth). It is important to recognize that severe accident analyses [13] indicate that the plenum does not always fully void when the active core voids; therefore, insertion of the plenum reactivity effect is dictated by the transient conditions and the void worth of the core alone is still relevant. Significant differences between diffusion and transport theory predictions are observed for voiding of the control rod channels. Whereas diffusion theory predicts a large decrease in the eigenvalue when the control rod channels are voided, all transport methods predict a control channel voiding effect that is slightly positive. This can be explained in view of the expected weaknesses of diffusion theory in quasi voided regions. It is expected that diffusion and transport models predict roughly the same spectral effects due to voiding of the control rod channels, whereas diffusion theory significantly overpredicts the leakage effect, resulting in a net negative worth in the framework of diffusion theory, and a null or slightly positive worth in transport theory.

The two higher order methods used in these calculations exhibit slightly different behaviors: whereas VARIANT predicts a significantly positive total voiding reactivity (~1.5$), VIM predicts a positive but almost null reactivity. The bias between the VIM and VARIANT results is generated in the active core void worth prediction, and similar differences are observed as progressively more regions are voided. This behavior infers that the difference between the VIM and VARIANT results is most likely caused by discrepancies in the spectral component (which dominates in the active core) while leakage effects (which dominate for all other regions) are similar. Because the spectral component is especially sensitive to small differences in the cross section data, it is expected the discrepancies are caused by the cross section data. The multigroup cross sections used in VARIANT were obtained through condensation and homogenization procedures which can not fully account for spectral and spatial flux perturbations in a full core model; the VIM cross sections do not take into account pin-cell heterogeneity and the VIM calculations presented here were performed at room temperature. Furthermore, the sodium void worth of a low void worth core is the difference of two large and almost equal components (spectral and leakage components), and a small deviation in one of these terms can result in a large relative misprediction of the net void worth. Thus, the results presented in this report indicate that even with the best data and methods available today, the uncertainty on the calculated worth of a low void worth core remains high.

Finally, the good agreement between results obtained from the simplified version of VARIANT and its advanced version is noteworthy, as it indicates that the faster version can be used for scoping studies. As expected, some differences in the leakage effects are observed between the P_0 and P_1 calculations; the P_0 method predicts a larger eigenvalue decrease for voiding of the plenum region (see Fig. 5). However, the difference between the two calculations is never greater than 0.2 % $\Delta k/(kk')$.

V. BENCHMARK HETEROGENEITY RESULTS AND DISCUSSION

The effects of steel heterogeneity and interstitial sodium on the sodium void reactivity were assessed using a series of continuous energy Monte Carlo calculations. This choice of computational technique was prompted by the following:

- Monte Carlo codes have the unique ability to model complex 3D geometries.

- continuous energy representations of cross sections can implicitly represent the effect of large spectral gradients, whereas multigroup calculations rely on user supplied regional dependent cross sections which might be particularly difficult to approximate for partial voiding cases under consideration in this benchmark effort.

A hexagonal-Z subassembly model consistent with the benchmark specifications was set up. The radial boundary conditions were purely reflective, to model an infinite array of subassemblies.

Two minor approximations were made:

-fission products were not modelled (see earlier discussion)

-all isotopes were at room temperature (300K)

These two approximations should not affect the validity of the following comparisons. A radially homogenized model was also set up; the homogenized compositions were obtained from volume weighting the heterogeneous compositions in the horizontal plane. The following six cases were run:

- case 1: heterogenous model, fully flooded

- case 2: heterogeneous model, voided flowing sodium, flooded interstitial sodium

- case 3: heterogeneous model, all sodium voided

- case 4: radially homogenized case 1

- case 5: radially homogenized case 2

- case 6: radially homogenized case 3

Table V indicates the corresponding k-effective (with one sigma uncertainties), voiding delta k's (with three sigma uncertainty ranges), and heterogeneity effects on voiding delta k's (defined as the difference between the heterogeneous and homogeneous values). A difference of 0.15% delta k is observed between the homogeneous and heterogeneous eigenvalue predictions for the flooded model; however, the fully voided eigenvalues are nearly identical. Thus, the heterogeneity effect on the full voiding worth is relatively important (reduction from 0.76% delta k to 0.60% delta k), and should be taken into account in full core calculations, where it would tend to reduce the overall void worth.

A surprising effect is the relative contributions of the flowing sodium and the interstitial sodium: they are of roughly the same magnitude in both the heterogeneous and homogeneous cases, even though the masses of sodium involved are in a ratio of 1:4. This effect is clearly unrelated to neutron streaming (as it is observed for the homogeneous model), and might be related to some non-linear spectral behavior (note that the interstitial contribution is calculated when the flowing sodium is already voided). Further investigation of this behavior is planned at ANL.

VI. CONCLUSIONS

The results presented in this paper were prepared for comparison with results from other participants to the IAEA International Benchmark. Several noteworthy results were pointed out. It was shown that, when higher order calculational techniques are used, the sodium void worth of the benchmark is calculated to be slightly positive for all six voided configurations. It was also shown that the uncertainty on calculated void worths of low void worth cores remains quite high, even when higher order methods are used.

Although the overall void worth of the benchmark configuration is very low, the reduction of the void worth to a near-zero value is achieved at the expense of performance, design, and possibly safety penalties [1]; the usefulness of the void worth reduction techniques must be evaluated in the context of overall safety of the reactor system [2]. Thus, the design goal of a near-zero void worth may be achieved at the expense of overall performance and safety.

REFERENCES

1. H. S. Khalil and R. N. Hill, "Evaluation of Liquid-Metal Reactor Design Options for Reduction of Sodium Void Worth," *Nuclear Science and Engineering*, **109**, 221 (1991).

2. P. A. Pizzica, R. A. Wigeland, and R. N. Hill, "Effects of Reducing the Sodium Void Worth on the Passive Safety Response of 900 MWt Liquid-Metal-Cooled Reactors to Various Unprotected Accidents," *Transactions of the American Nuclear Society*, **66**, 315 (1992).

3. R. N. Hill, M. Kawashima, K. Arie, and M. Suzuki, "Calculational Benchmark Comparisons for a Low Sodium Void Worth Actinide Burner Core Design," 1992 Topical Meeting on Advances in Reactor Physics, Charleston, South Carolina, March 8-11, 1992, p. 1-313.

4. IAEA - Commission of the European Communities "Specification of the Calculation Model of a Fast Power Reactor with Sodium Void Reactivity Close to Zero," Vienna, Brussels (1992).

5. H. Henryson II, B. J. Toppel, and C. G. Stenberg, "MC2-2: A Code to Calculate Fast Neutron Spectra and Multigroup Cross Sections," ANL-8144, Argonne National Laboratory (June 1976).

6. W. M. Stacey Jr. et al., "A New Space-Dependent Fast-Neutron Multigroup Cross-Section Capability," *Transactions of the American Nuclear Society*, **15**, 292 (1972).

7. B. J. Toppel, "A User's Guide to the REBUS-3 Fuel Cycle Analysis Capability," ANL-83-2, Argonne National Laboratory (March 1983).

8. R. N. Blomquist, "VIM", Procs of the Topical Conference on Advances in Mathematics, Computations, and Reactor Physics, Pittsburgh, PA, April 1991, p30.4, 2-2.

9. C. Carrico, G. Palmiotti, and E. Lewis, "Three Dimensional Nodal Transport Methods for Cartesian, Triangular, and Hexagonal Criticality Calculations," *Nuclear Science and Engineering*, **111**, 168 (1992).

10. C. Carrico, E. Lewis, and G. Palmiotti, "Reduced Angular Trial Function Set for the Variational Nodal Method," *Transactions of the American Nuclear Society*, **65**, 200 (1992).

11. G. Palmiotti, C. Carrico, E. Lewis, "Generalization of the Variational Nodal Method to Include Anisotropic Scattering," *Transactions of the American Nuclear Society*, **66**, 271 (1992).

9. K. L. Derstine, "DIF3D: A Code to Solve One-, Two-, and Three-Dimensional Finite-Difference Diffusion Theory Problems," ANL-82-64, Argonne National Laboratory (April 1984).

13. A. M. Tentner "SAS4A Analysis of Unprotected Loss-of-Flow Accidents in a Metal-Fuel Reactor," *Transactions of the American Nuclear Society*, **66**, 573 (1992).

FIGURE 1.

IAEA–92 BENCHMARK, LOWER CORE MIDPLANE
Peak Power Density by Assembly, kw/liter

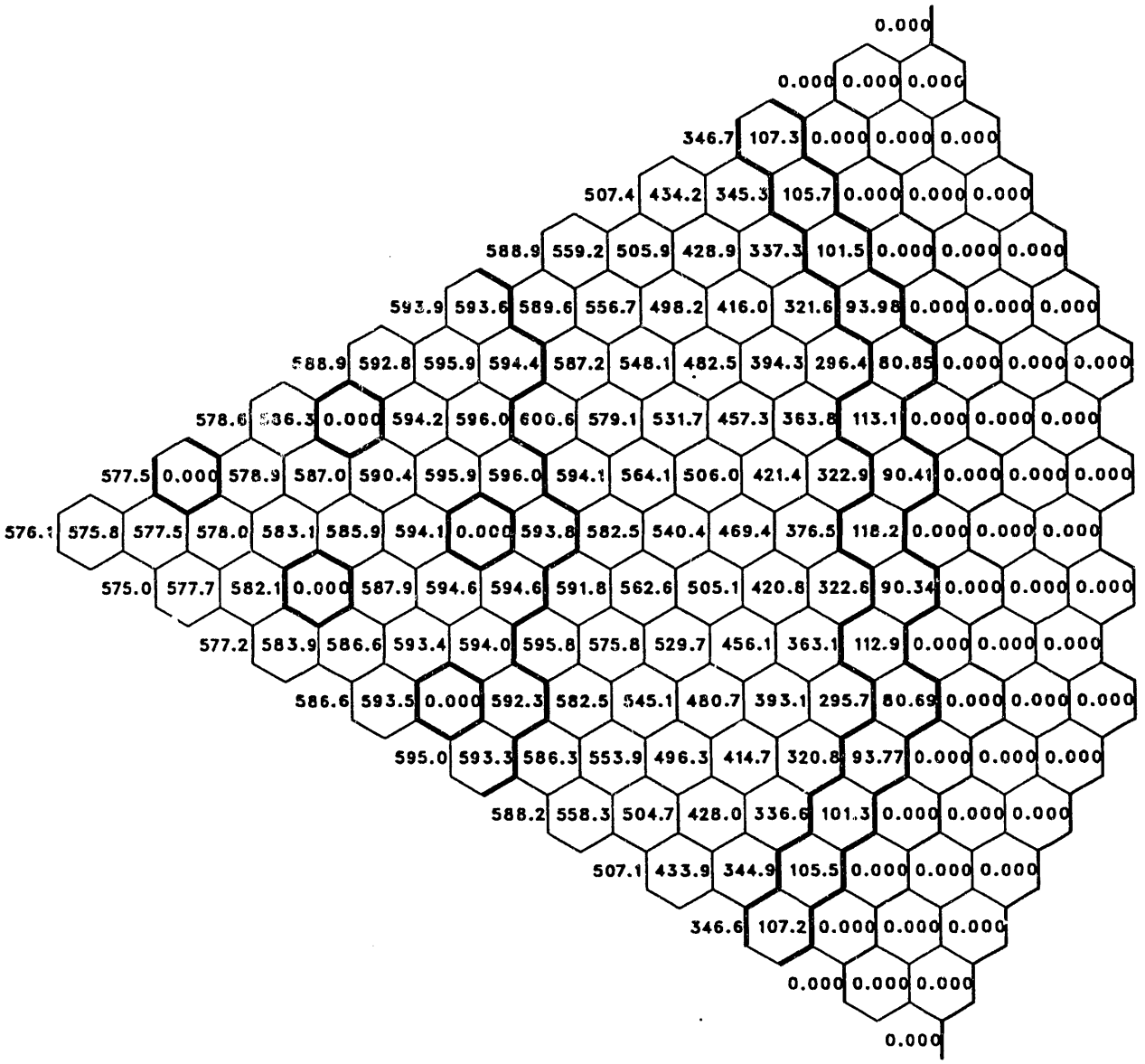

FIGURE 2.

IAEA–92 BENCHMARK, UPPER CORE MIDPLANE
Peak Power Density by Assembly, kw/liter

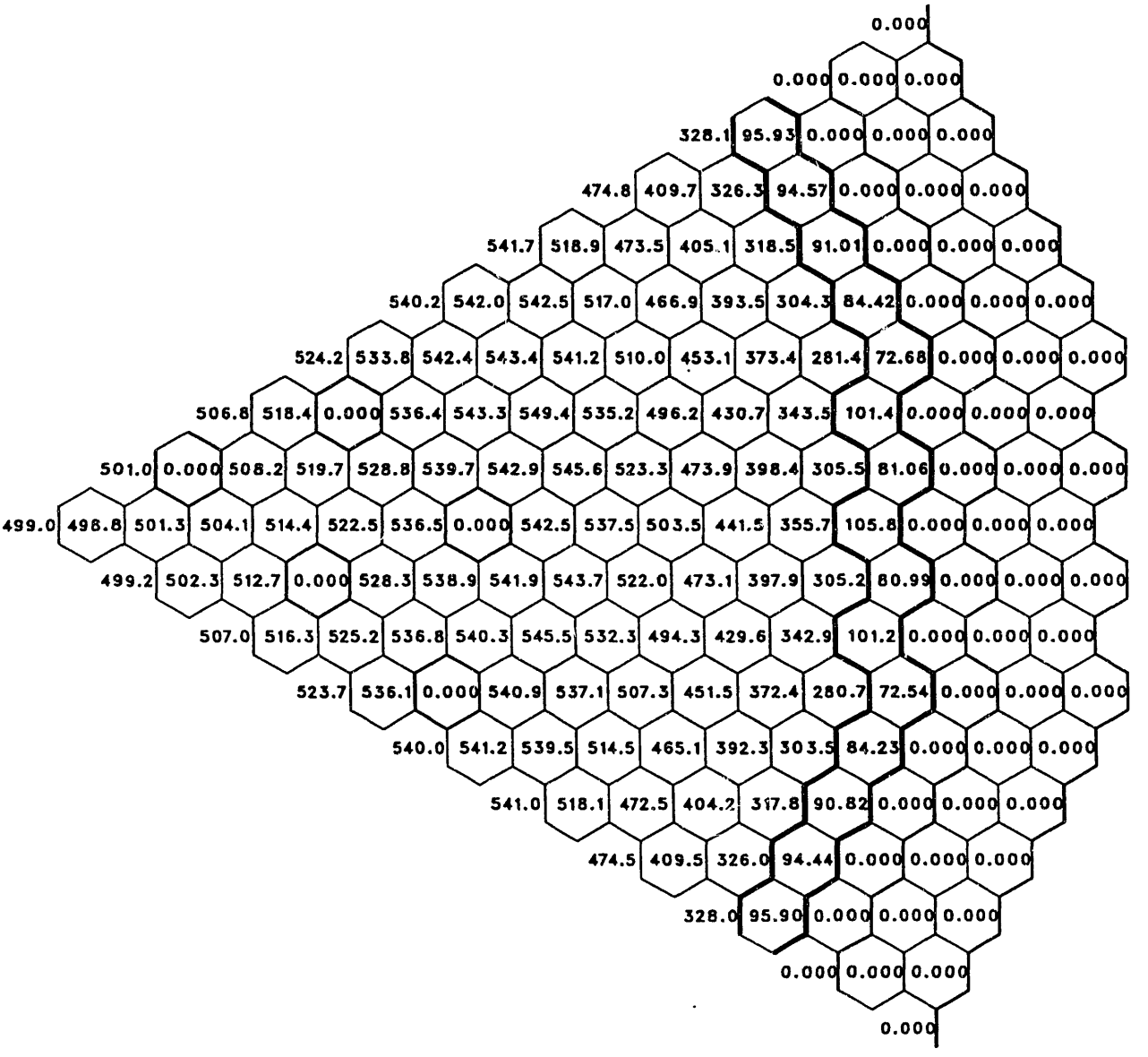

FIGURE 3.

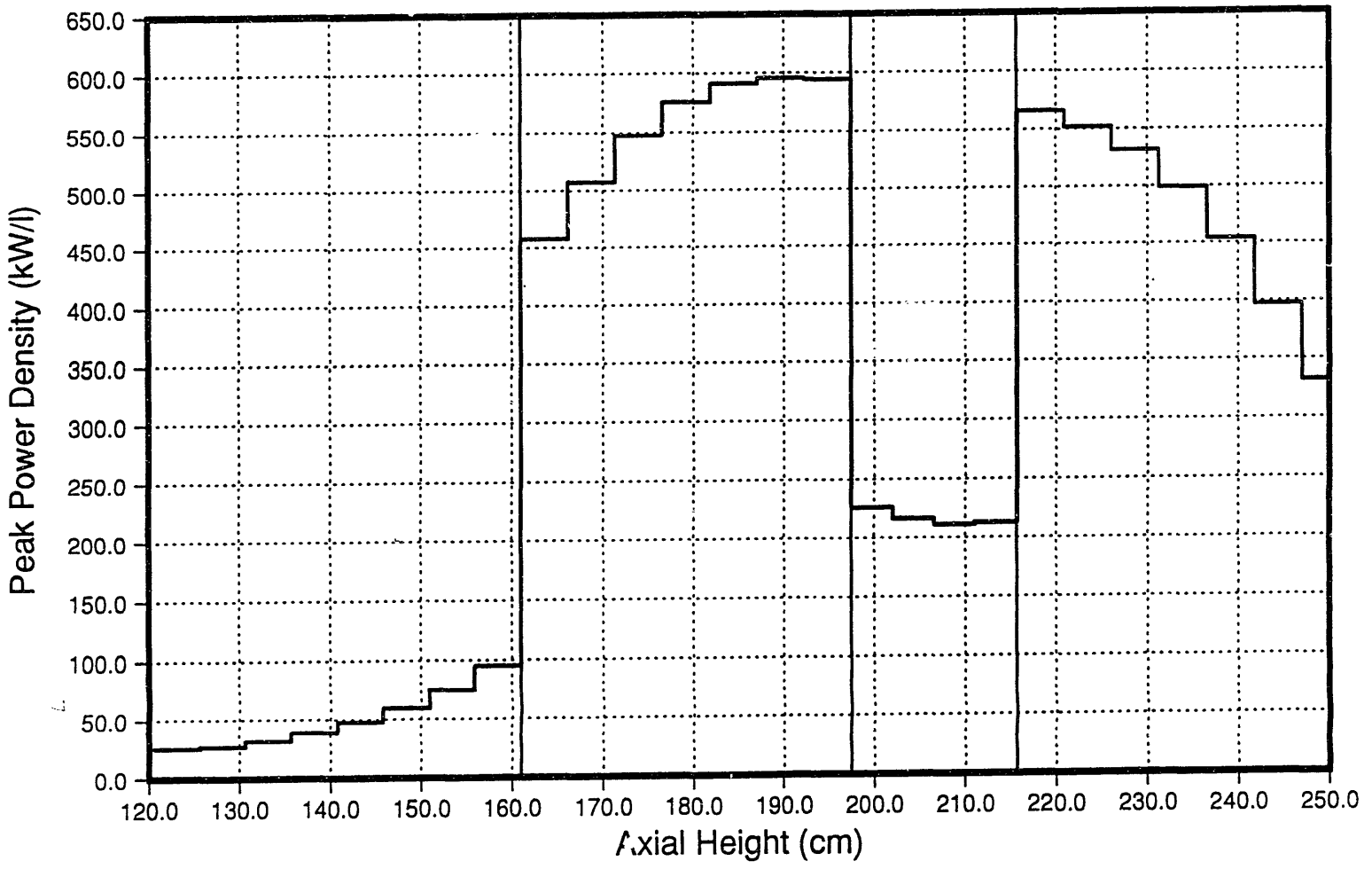
Axial Power Distribution - Central Assembly
Peak Power Density (kW/l)
650.0
600.0
550.0
500.0
450.0
400.0
350.0
300.0
250.0
200.0
150.0
100.0
50.0
0.0
120.0
130.0
140.0
150.0
160.0
170.0
180.0
190.0
200.0
210.0
220.0
230.0
240.0
250.0
Axial Height (cm)

FIGURE 4.

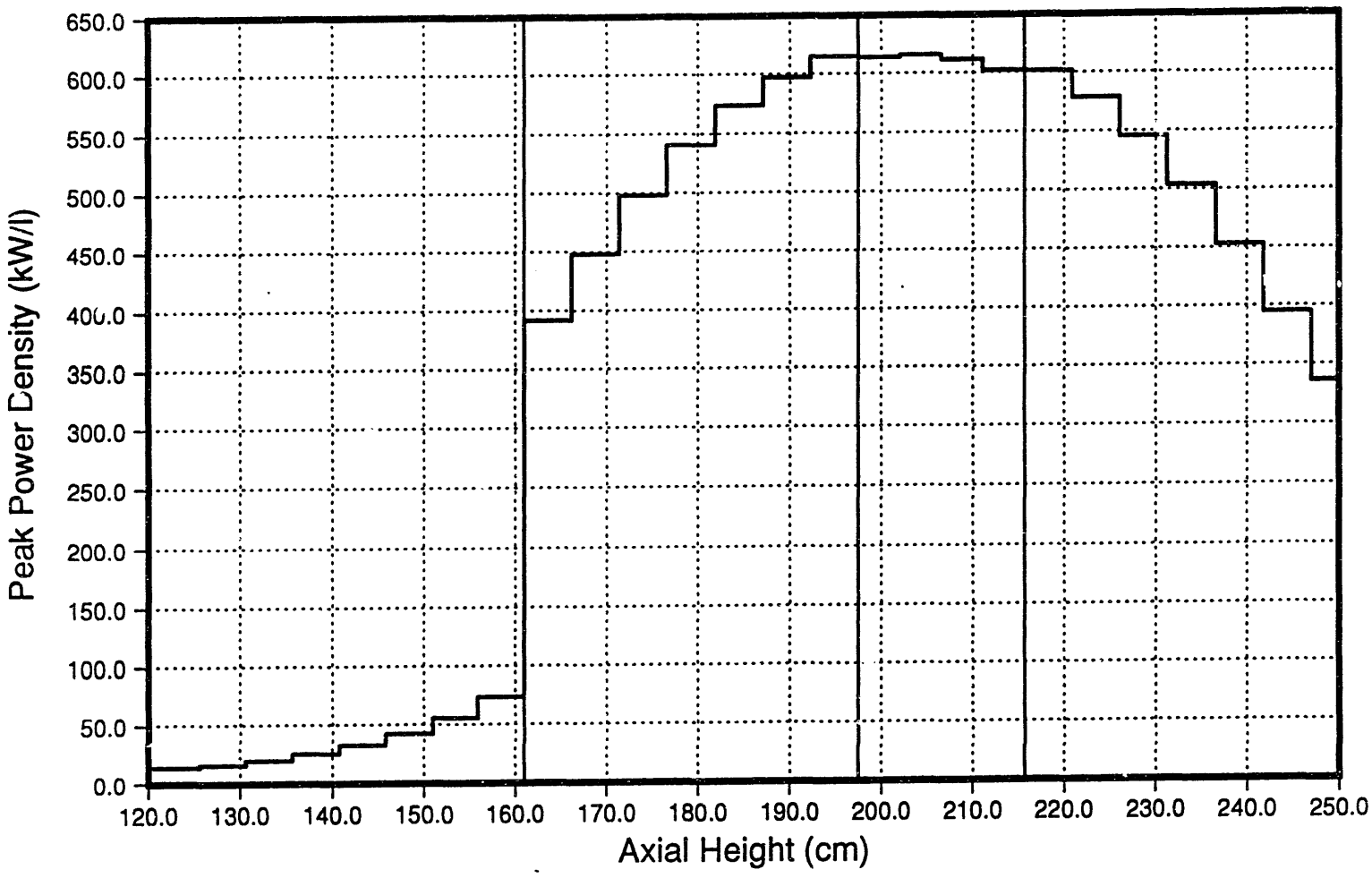
Axial Power Distribution - Outer Assembly
Peak Power Density (kW/l)
650.0
600.0
550.0
500.0
450.0
400.0
350.0
300.0
250.0
200.0
150.0
100.0
50.0
0.0
120.0
130.0
140.0
150.0
160.0
170.0
180.0
190.0
200.0
210.0
220.0
230.0
240.0
250.0
Axial Height (cm)

FIGURE 5: IAEA92 DELTA K

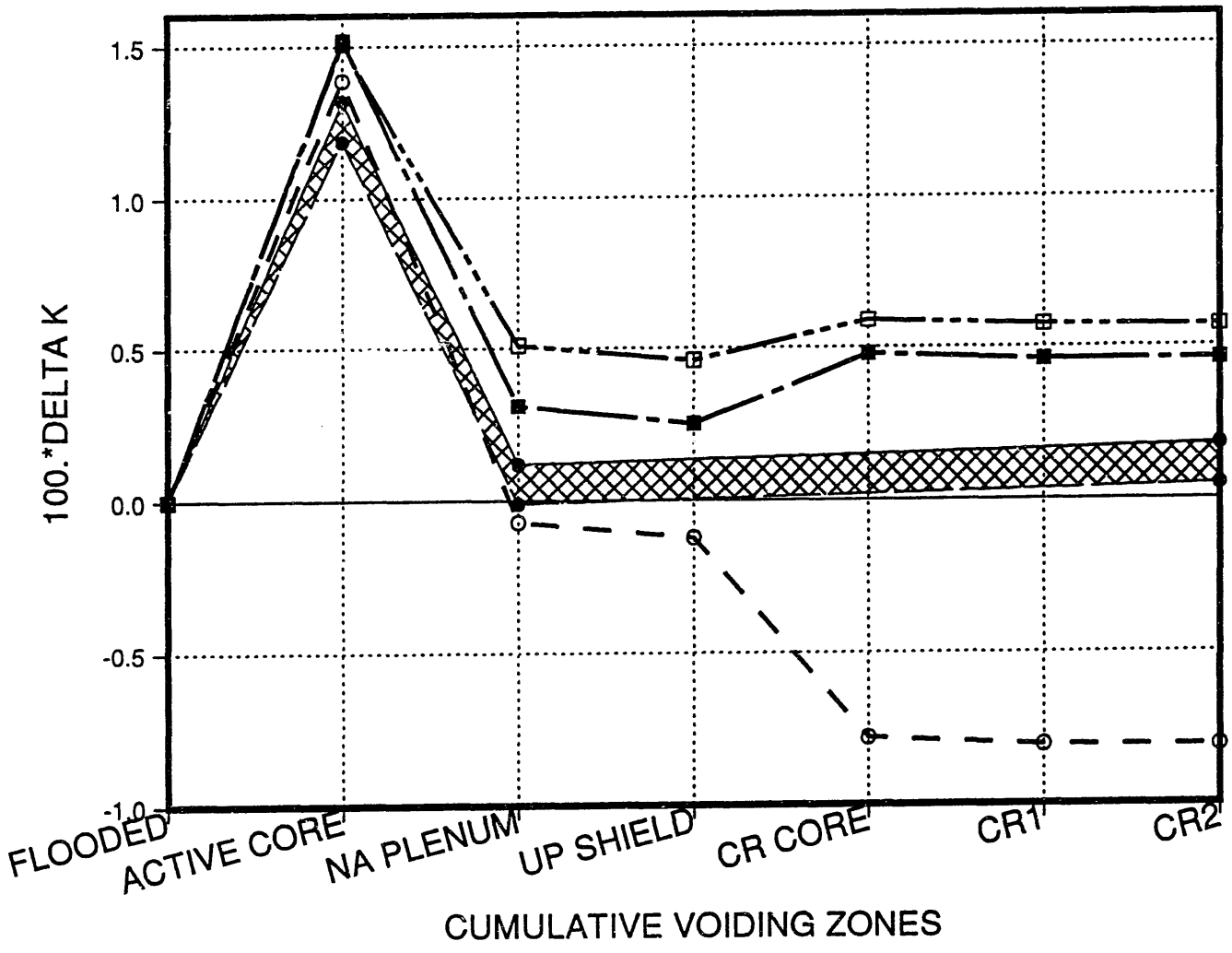

Legend

- MONTE CARLO, CORRECTED FOR FISSION PRODUCTS, +3 SIGMA
- MONTE CARLO, CORRECTED FOR FISSION PRODUCTS, -3 SIGMA
- DIF3D NODAL
- VARIANT P0*, REDUCED ANGULAR TRIAL FUNCTIONS
- VARIANT P1

Table I. Comparison of Criticality and Sodium Void Worth Predictions
(With Fission Products)

	Diffusion Theory		Nodal Transport	
	Finite Diff.	Nodal	P0*	P1
k_{eff}, Flooded	0.9953	0.9942	1.0033	1.0029
Case #1, Voiding of Active Core Only (including internal breeder zone)				
k_{eff}, Voided	1.0093	1.0081	1.0185	1.0180
Sodium Void Worth, %Δk/(kk')	1.390	1.387	1.487	1.478
Case #2, Voiding of Active Core, pin steel plugs, and sodium plenum				
k_{eff}, Voided	0.9948	0.9935	1.0063	1.0080
Sodium Void Worth, %Δk/(kk')	-0.051	-0.071	0.297	0.507
Case #3, Voiding of Active Core, pin steel plugs, sodium plenum, and upper axial shield				
k_{eff}, Voided	0.9942	0.9930	1.0058	1.0075
Sodium Void Worth, %Δk/(kk')	-0.111	-0.122	0.248	0.459
Case #4, Voiding of Drivers as in Case #3 and CR follower				
k_{eff}, Voided	0.9880	0.9864	1.0081	1.0088
Sodium Void Worth, %Δk/(kk')	-0.740	-0.795	0.475	0.581
Case #5, Voiding of Drivers as in Case #3 CR follower, and lower absorber zone				
k_{eff}, Voided	0.9877	0.9862	1.0079	1.0086
Sodium Void Worth, %Δk/(kk')	-0.768	-0.816	0.455	0.568
Case #6, Voiding of Drivers as in Case #3 CR follower, and absorber zone				
k_{eff}, Voided	0.9877	0.9861	1.0079	1.0086
Sodium Void Worth, %Δk/(kk')	-0.771	-0.826	0.455	0.565

*Corrected P_0 scattering matrices with reduced angular trial functions

Table II. Comparison of Criticality and Sodium Void Worth Predictions
(Without Fission Products)

	Diffusion, Finite Diff.	Transport, Nodal*	Monte Carlo (1σ)
k_{eff}, Flooded	1.0145	1.0226	1.02383 (0.00013)
Case #1, Voiding of Active Core Only (including internal breeder zone)			
k_{eff}, Voided	1.0259	1.0353	1.03389 (0.00018)
Sodium Void Worth, %Δk/(kk')	1.102	1.200	0.950 (0.022)
Case #2, Voiding of Active Core, pin steel plugs, and sodium plenum			
k_{eff}, Voided	1.0109	1.0226	1.02130 (0.00018)
Sodium Void Worth, %Δk/(kk')	-0.351	0.000	-0.242 (0.022)
Case #3, Voiding of Active Core, pin steel plugs, sodium plenum, and upper axial shield			
k_{eff}, Voided	1.0102		
Sodium Void Worth, %Δk/(kk')	-0.410		
Case #4, Voiding of Drivers as in Case #3 and CR follower			
k_{eff}, Voided	1.0032		
Sodium Void Worth, %Δk/(kk')	-1.103		
Case #5, Voiding of Drivers as in Case #3 CR follower, and lower absorber zone			
k_{eff}, Voided	1.0029		
Sodium Void Worth, %Δk/(kk')	-1.132		
Case #6, Voiding of Drivers as in Case #3 CR follower, and absorber zone			
k_{eff}, Voided	1.0029	1.0236	1.02123 (0.00018)
Sodium Void Worth, %Δk/(kk')	-1.134	0.096	-0.249 (0.022)

*Corrected P_0 scattering matrices with reduced angular trial functions

Table III. Breakdown of Sodium Void Worth Components
(Case #6, Voiding of Drivers and Control Rods, Finite Diff. Diffusion Theory)

all values are %Δk/(kk')	Total	Spectral	Leakage	Capture
Zone #1 (Upper Inner Core)	0.175	0.339	-0.204	0.046
Zone #2 (Lower Inner Core)	0.415	0.473	-0.117	0.068
Zone #3 (Upper Outer Core)	-0.024	0.379	-0.451	0.048
Zone #4 (Middle Outer Core)	0.224	0.339	-0.156	0.042
Zone #5 (Lower Outer Core)	0.132	0.499	-0.428	0.062
Total Driver	0.922	2.028	-1.356	0.266
Zone #6 (Internal Blanket)	0.323	0.296	-0.005	0.037
Total Active Core	1.245	2.324	-1.361	0.303
Zone #9 (Pin Steel Plugs)	-0.102	0.034	-0.138	0.001
Zone #10 (Sodium Plenum)	-1.321	0.364	-1.695	0.010
Zone #11 (Upper Axial Shield)	-0.038	0.018	-0.056	0.000
Total Fuel Assembly Voiding	-0.216	2.740	-3.250	0.314
Zone #29 (CR Followers)	-0.537	0.402	-0.968	0.029
Zone #27 (Compensating Rod)	-0.001	0.001	-0.002	0.000
Zone #28 (Compensating Rod)	-0.008	0.012	-0.020	0.000
Zone #36 (Safety Rod)	-0.001	0.000	-0.001	0.000
Zone #37 (Safety Rod)	-0.009	0.008	-0.018	0.000
Total Control Assembly Voiding	-0.555	0.423	-1.009	0.029
Whole Core Voiding	-0.771	3.163	-4.259	0.343

Table IV. Calculated Neutronic Performance Characteristics

Breeding Ratio	1.0038
Driver	0.6093
Internal Blanket	0.0892
Axial Blanket	0.1315
Radial Blanket	0.1738
Burnup Swing, %Δk/(kk'), 30-day cycle	0.524
Peak Linear Power, W/cm	451
Power Peaking Factor	1.443
Regional Power Fraction, %	
Driver	90.1
Internal Blanket	3.7
Axial Blanket	3.1
Radial Blanket	3.1
Initial Inventory, kg	
Fissile Pu	2,048
Total Heavy Metal	25,485
Control Rod Worths, %Δk/(kk')	
Compensating Rods	3.93
Safety Rods	3.70

Table V: Monte Carlo Calculation of Heterogeneity Effects

Case	Number of histories	k-effective (1 sigma)	delta k from	%delta k (1 sigma)	Heterogeneity effect % (1 sigma)
1 het- all flooded	9,500,000	1.07837 (.00017)			
2 het- flowing Na voided	4,500,000	1.08157 (.00029)	case 1	.320 (.034)	
3 het- all voided	9,500,000	1.08440 (.00017)	case 1 case 2	.603 (.024) .283 (.034)	
4 hom- all flooded	9,500,000	1.076814 (.00017)			
5 hom- flowing Na voided	4,500,000	1.080198 (.00029)	case 4	.338 (.034)	.018 (.048)
6 hom- all voided	9,500,000	1.08439 (.00017)	case 4 case 5	.758 (.024) .419 (.034)	.155 (.034) .136 (.048)

END

DATE
FILMED
5/7/93